Airborne Measurements of Rain and the Ocean Surface Backscatter Response at C- and Ku-band

Daniel Esteban Fernandez, Paul S. Chang*, James R. Carswell†, Robert F. Contreras and Stephen J. Frasier‡

* Office of Research and Applications
NOAA / NESDIS,
Camp Springs, MD 20746

† Remote Sensing Solutions
Barnstable, MA 02630

‡ Microwave Remote Sensing Laboratory
University of Massachusetts, Amherst, MA 01003

***Abstract*— During the 2002, 2003, and 2004 Hurricane seasons, and the 2005 Ocean Winds and Rain Winter Experiment, the University of Massachusetts (UMass) installed two instruments on the NOAA N42RF WP-3D research aircraft: the Imaging Wind and Rain Airborne Profiler (IWRAP) and the Simultaneous Frequency Microwave Radiometer (SFMR). IWRAP is a dual-band (C- and Ku), dual-polarized pencil-beam airborne radar that profiles the volume backscatter and Doppler velocity from rain and that also measures the ocean backscatter response. It simultaneously profiles along four separate incidence angles while conically scanning at 60 RPM. SFMR is a C-band nadir viewing radiometer that measures the emission from the ocean surface and intervening atmosphere simultaneously at six frequencies. It is designed to obtain the surface wind speed and the column average rain rate. Both instruments have previously been flown during hurricane seasons 2002, 2003 and 2004.**

Spectral techniques can been used to differentiate the contributions of the volume backscatter from rain from the ocean surface backscatter. Initial results from the Winter 2005 datasets are presented. Attenuation from rain is also particularly important at high microwave frequencies such as Ku-band. Thanks to IWRAP's profiling capabilities, Ku-band attenuation models and dropsize distribution (DSD) parameters of the observed precipitation from dual-wavelength techniques within tropical cyclones are presented.

I. Introduction

IWRAP, the Imaging Wind and Rain Airborne Profiler, is a high-resolution, dual-band (C- and Ku-band), dual-polarized, pencil-beam radar that profiles the Doppler velocity and volume backscatter from rain and measures the ocean backscatter response at 15 to 120 m range resolution. [1]. Developed by the University of Massachusetts with the support of Remote Sensing Solutions, and funded by NOAA/NESDIS, NASA/JPL and ONR, the system operates simultaneously at four separate incidence angles (covering an effective continuous swath of 25 to 50 degree incidence) while conically scanning at 60 RPM. SFMR, the Simultaneous Frequency Microwave Radiometer, is a C-band nadir vieweing radiometer that measures the emission from the ocean surface and atmosphere simultaneously at six separate frequencies (approximately ranging from 4 to 7 GHz). It is used operationally to provide continuous estimates of the surface wind speed and the column average rain rate [2].

During the 2001, 2002 and 2003, the UMass IWRAP instrument was respectively built, tested, and deployed aboard the NOAA WP-3D hurricane research and reconnaissance aircraft. Since then, IWRAP has participated every year in the NOAA/NESDIS Hurricane Ocean Winds and Rain Experiments, the NOAA/NESDIS Winter Experiments, and the ONR CBLAST Hurricane Program. During these fields experiments, dozens of missions have been flown through winter extratropical storms at high latitudes, as well as tropical storms and hurricanes (such as Gustav, Isidore and Lili in 2002, Fabian and Isabel in 2003, and Frances, Ivan and Jeanne in 2004), during various phases of these systems. All the IWRAP data was acquired with coincident SFMR measurements and hundreds of dropsonde and buoy in-situ measurements. In 2005, the IWRAP instrument was upgraded to acquire raw data.

In this paper, we present initial results from these datasets, which establish the grounds to ultimately analyze and quantify the impact of rain on the ocean surface backscatter response. The structure is as follows: we first present the use of spectral techniques with the 2005 Winter data, which allows to individuate and separate the contributions of the volume backscatter from rain from the ocean surface backscatter. The second section describes the use of the coincident dual-wavelength measurements to derive an attenuation model and rainfall rate estimates. Finally, the last section uses these results to derive a two-parameter drop-size distribution within tropical cyclones.

II. Ocean and rain spectra

The IWRAP system collected raw data for the first time during the 2005 winter experiment. The purpose of the upgrade was to address one of the fundamental limitations of pulse-pair processing, which was implemented on the FPGAs of the instrument's data acquisition system. The limitation comes from the incorrect estimation of the Doppler moments (mean and spectral width) when more than one contribution exists in the Doppler spectrum. For the case of any radar profiling the atmosphere and the ocean surface, the responses from volume backscatter from rain, surface backscatter from the ocean surface, and nadir returns (in non nadir-looking systems) can simultaneously contribute to the measurements [3] [4]. Given the fact that such contributions will typically be centered in different positions within the span of the full Doppler spectrum, the pulse-pair estimates will estimate a Doppler velocity mean which is a power-weighted combination of the individual Doppler velocity means of each one of the contributions. The spectral measurements provide instead the means to individuate the different contributions. Moreover, the ocean spectral response can be modelled under all wind conditions and in both rain and rain-free conditions. Rain processes can be characterized from the dual-wavelength measurements, as it will be discussed in the next section. The exact knowledge of both contributions thus allows to precisely quantify the impact of rain on the ocean backscatter on the spectral response as well as in the integrated power.

Report Documentation Page

Form Approved
OMB No. 0704-0188

1. REPORT DATE **25 JUL 2005**	2. REPORT TYPE **N/A**	3. DATES COVERED **-**
4. TITLE AND SUBTITLE **Airborne Measurements of Rain and the Ocean Surface Backscatter Response at C- and Ku-band**		5a. CONTRACT NUMBER 5b. GRANT NUMBER 5c. PROGRAM ELEMENT NUMBER
6. AUTHOR(S)		5d. PROJECT NUMBER 5e. TASK NUMBER 5f. WORK UNIT NUMBER
7. PERFORMING ORGANIZATION NAME(S) AND ADDRESS(ES) **Office of Research and Applications NOAA / NESDIS, Camp Springs, MD 20746**		8. PERFORMING ORGANIZATION REPORT NUMBER
9. SPONSORING/MONITORING AGENCY NAME(S) AND ADDRESS(ES)		10. SPONSOR/MONITOR'S ACRONYM(S) 11. SPONSOR/MONITOR'S REPORT NUMBER(S)

12. DISTRIBUTION/AVAILABILITY STATEMENT
Approved for public release, distribution unlimited

13. SUPPLEMENTARY NOTES
See also ADM001850, 2005 IEEE International Geoscience and Remote Sensing Symposium Proceedings (25th) (IGARSS 2005) Held in Seoul, Korea on 25-29 July 2005. , The original document contains color images.

14. ABSTRACT

15. SUBJECT TERMS

16. SECURITY CLASSIFICATION OF:			17. LIMITATION OF ABSTRACT	18. NUMBER OF PAGES	19a. NAME OF RESPONSIBLE PERSON
a. REPORT **unclassified**	b. ABSTRACT **unclassified**	c. THIS PAGE **unclassified**	**UU**	**4**	

Standard Form 298 (Rev. 8-98)
Prescribed by ANSI Std Z39-18

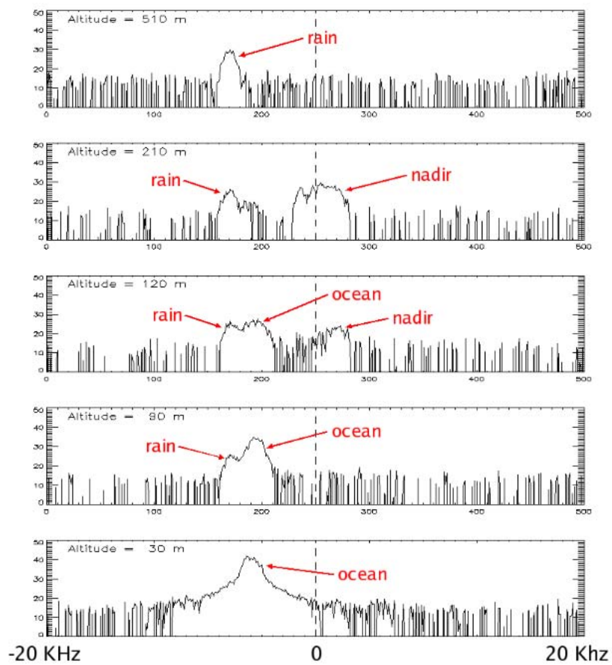

Fig. 1. Doppler spectra at altitudes ranging from 500 to 30 m at a fixed azimuth angle are shown. The different contributions from rain, nadir return and ocean surface backscatter are clearly indicated.

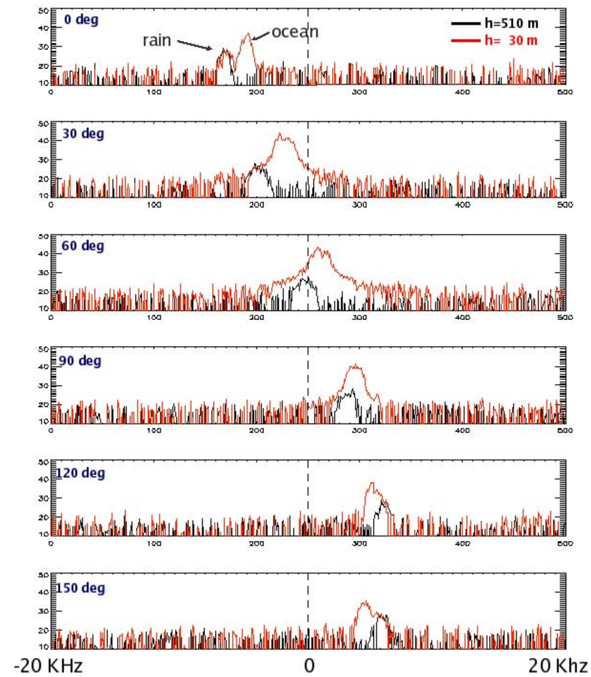

Fig. 2. Doppler spectra for half an azimuthal scan at two altitudes (500 and 30 m) are shown. The different contributions from rain and ocean surface backscatter are indicated.

Figure 1 shows the derived Doppler spectra at altitudes ranging from 30 to 500 m at a fixed azimuth angle (corresponding to the downwind look direction) and one incidence angle (40 degrees incidence) in the presence of light rain (less than 10 mm·hr^{-1}) and wind speeds below 20 m·s^{-1}. The figure clearly shows that the rain contribution, shown alone at an altitude of 510 m, is first contaminated by the nadir return at 210 m, and then by the ocean surface backscatter below 120 m. In this situation it is clear that the nadir contributions can be easily removed by filtering out the undesired part of the spectrum for the lowest boundary layer. The relatively low winds place both ocean and rain spectral components close enough as to make the filtering a non viable solution. However, the ocean response at 0 m above the ocean's surface can be used to model the responses at other altitudes to substract them from the obtained spectrum. This approach is currently being evaluated. In the presence of stronger winds, like the ones found in the context of tropical cyclones, both contributions are expected to be placed further apart from each other, and thus filtering could be used, although only for some azimuthal positions along the scan; as figure 2 shows, the ocean backscatter response (shown at 30 m, where it predominates over the contribution from the rain) overlays the rain spectra for some of the azimuthal positions. Depending on the technique employed, however, the rain spectra does not need to be individuated at all azimuthal positions in order to retrieve the boundary layer winds.

III. Dual-wavelength attenuation from precipitation

Many remote sensing techniques have been developed for precipitation rate (R_r) estimation. These methods can be broken down into single and multi-parameter approaches. One of the most commonly used single parameter techniques relates the radar reflectivity factor Z (i.e. volume backscatter measurements) to R_r, usually by means of a power law. Unfortunately, the Z-R_r relationship can vary significantly for different types of precipitation and for different climates. Battan lists more than 60 different Z-R_r relationships based on drop-size distribution measurements made in different climatic regions [9]. To assume that is it possible to find such a Z-R relationship is to imply that some of the drop-size distribution (DSD) parameters are not independent variables.

Multi-parameter approaches are better suited to retrieve precipitation rate. One approach is to acquire volume backscatter measurements at two different electromagnetic wavelengths, a long wavelength (in our case, C-Band) that is virtually not attenuated, and a shorter wavelength (Ku-band) that is attenuated. From both these measurements, the path averaged specific attenuation, K_s, in dB·km^{-1}, can be determined from the reflectivity factors at the two frequencies and over two different ranges, as given by:

$$K_s = \frac{1}{2(r_2 - r_1)}\left[Z_c(r_2) + Z_{ku}(r_1) - (Z_(r_1) - Z_{ku}(r_2))\right]. \quad (1)$$

where r_1 and r_2 are the ranges and $Z_c(r_i)$ and $Z_{ku}(r_i)$ denote the reflectivity factors in dBZ at range r_i at C- and Ku-band, respectively. From measurements of K_s and Z, a two parameter drop-size distribution, $N(D)$, can be calculated, and from this information, the precipitation rate can be determined. Note that such a method still relies on measuring Z, but provides another degree of freedom to better describe the drop-size distribution that is being observed. Moreover, the attenuation estimate is independent of the radar calibration. However, it requires that no hail is present between r_1 and r_2; otherwise, K_s will remain the average attenuation along the path.

Figure 3 presents a scatter plot of the specific attenuation versus the SFMR rain rate estimates. The differential reflectivity is obtained from reflectivity measurements at flight level and 1 km range distance. Two models derived by Atlas [5] at 10^{o}C and 40^{o}C are overlaid. From

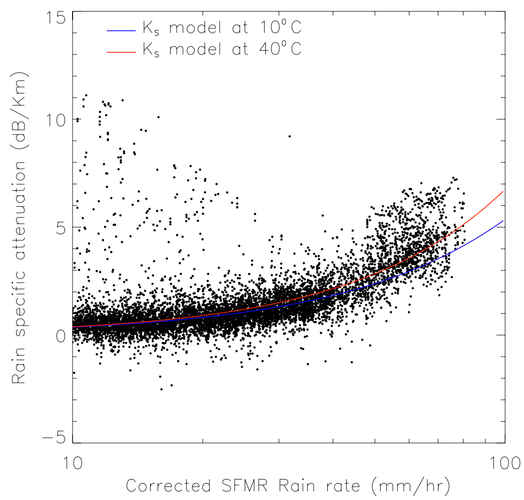

Fig. 3. Scatter plot of specific attenuation measurements from dual-wavelength techniques obtained during three flights through hurricane Isabel (2003) versus the SFMR rainfall rate estimates. Atlas' models of the specific attenuation at 10^{o}C and 40^{o}C are overlaid. The derivation of the corrected SFMR rain rate is described in [8].

these measurements, a power law relating the specific attenuation and the SFMR rate can be derived. The obtained relationship is:

$$K_s = 0.02 R_r^{1.276}. \quad (2)$$

The 1-σ errors for the fitted parameters are $1x10^{-3}$ for the coefficient and $1.4x10^{-2}$ for the exponent. The derived K-R relationship can now be used to obtain rainfall rates from the dual-wavelength IWRAP reflectivity measurements. Figure 4 presents an instance of such measurements corresponding to a flight through Hurricane Isabel (2003). As the figure shows, the agreement is excellent except at the highest rain rates ($>$ 70 mm·hr^{-1}), where the IWRAP estimates predict a greater rainfall rate than SFMR. Possible reasons for the discrepancy are associated to: 1) the SFMR rainfall rate estimates are column averaged, while the IWRAP uses only the attenuation within the first km from the aircraft in deriving the estimates. These volumes are different and for the most intense rain rates this difference can be significant. Its cone geometry makes SFMR more sensitive to rain rates closer to the surface; and 2) IWRAP is a much higher resolution instrument, and it is likely to see higher rain rates since SFMR will smooth the precipitation events and miss high resolution events.

IV. Two-parameter Drop-size distributions

By using both the attenuation and reflectivity measurements, a two-parameter DSD can be derived. We will hereafter consider an exponential distribution of the form

$$N(D) = N_0 e^{-\Lambda D}, \quad (3)$$

where N_0 and Λ are functions of the diameter of the hydrometers, D. With this assumption, the specific attenuation can be expressed by

$$K_s = 4.34x10^3 N_0 \int_D e^{-\Lambda D} \sigma_e(D) dD, \quad (4)$$

where K_s is in dB·km^{-1} and σ_e is the total attenuation or extinction cross section. The expression can be approximated by a power law [6]. On the other hand, when D is small compared to the electromagnetic wavelength λ (i.e. Rayleigh scattering, D $<$ λ/8), the radar reflectivity factor can be expressed as

$$Z = \int_0^\infty N(D) D^6 dD. \quad (5)$$

For both expressions, the integration can be performed using the exponential distribution given by eq. 3. Figures 5 and 6 show the resulting Λ and N_0 parameters from the observations acquired during three flights through Hurricane Isabel, where the reflectivity measurements at C-band and flight level have been used for eq. 5.

N_0 values have been suggested as $2.2x10^4$ m^{-3}·mm^{-1} for rain, 10^5 m^{-3}·mm^{-1} for snow and $4x10^3$·m^{-3} mm^{-1} for graupel [7]. Figure 6 indicates that all these three forms are present for rain rates mostly below 40 mm·hr^{-1}. Above that, the median N_0 is of the order of $2.8x10^4$ m^{-3}·mm^{-1}, indicating the presence of mostly rain only. The median mass diameter, D_0, can then be obtained by applying the exponential DSD under consideration into its defining equation:

$$\int_0^{D_0} D^3 e^{-\Lambda D} dD = \frac{1}{2} \int_0^\infty D^3 e^{-\Lambda D} dD. \quad (6)$$

Figure 7 shows the derived median mass diameter for the same observations.

These results suggest that correcting the ocean backscatter response from attenuation becomes an extremely difficult task even at the lower rainfall rates (above 10 mm·hr^{-1}), given the large range of raindrop diameters. Even in the situations where the rainfall rate is low enough so that the impact of the attenuation is not large and the impact of the rain drops on the ocean surface is believed not to have too much of an effect for the retrieval of the ocean wind vector, the broad spread in the median diameters would make any correction method prone to large errors.

V. Summary

For the first time, IWRAP raw data measurements of the atmospheric boundary layer and the ocean surface have been acquired. The use of spectral techniques to identify and separate ocean and rain backscatters allows us to: 1) derive the ocean spectral response in saturation; 2) analyze the impact of rain on the ocean backscatter with an exact knowledge of both contributions; and 3) remove the ocean backscatter response to derive the ABL winds down to the surface. Also, from the dual-wavelength measurements of rain, an attenuation versus rain rate model has been derived, and rainfall rate

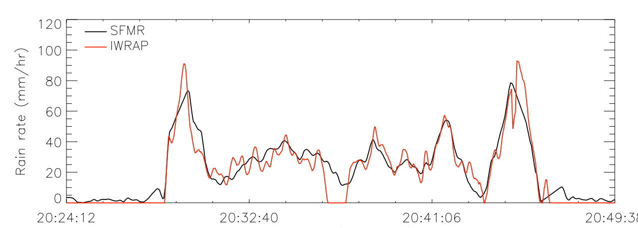

(a)

Fig. 4. Derived rainfall rate estimates from IWRAP measurements. The SFMR estimates are also shown. The measurements correspond to an eye-wall penetration through Hurricane Isabel on September 12th, 2003.

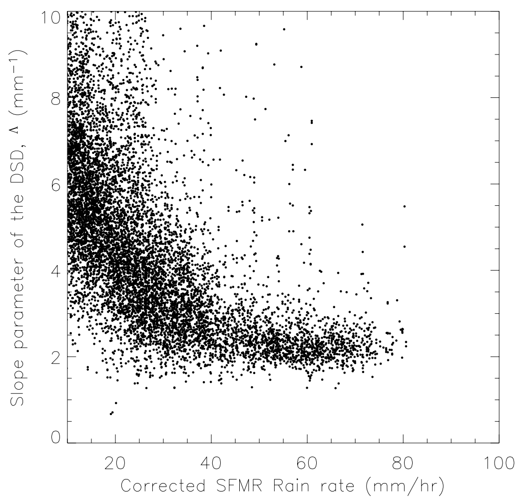

Fig. 5. Scatter plot of the slope of the DSD, Λ, versus the corrected SFMR rainfall rate estimates obtained from the C-band 30 degrees incidence flight level reflectivity measurements acquired during the Isabel flights on the 12th, 13th and 14th of September.

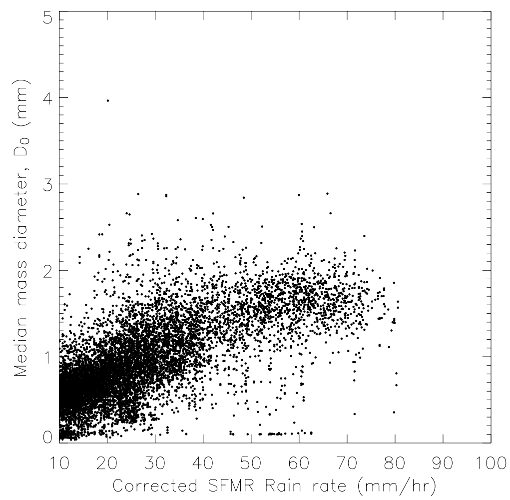

Fig. 7. Scatter plot of the DSD slope, D_0, versus the corrected SFMR rainfall rate estimates obtained from the C-band 30 degrees incidence flight level reflectivity measurements acquired during the Isabel flights on the 12th, 13th and 14th of September.

estimates through hurricane passes have been presented. Drop size distribution parameters have also been extracted, indicating the difficulties associated with the correction of the ocean surface backscatter response in the presence of rainfall rates above 10 mm$\cdot$hr^{-1}.

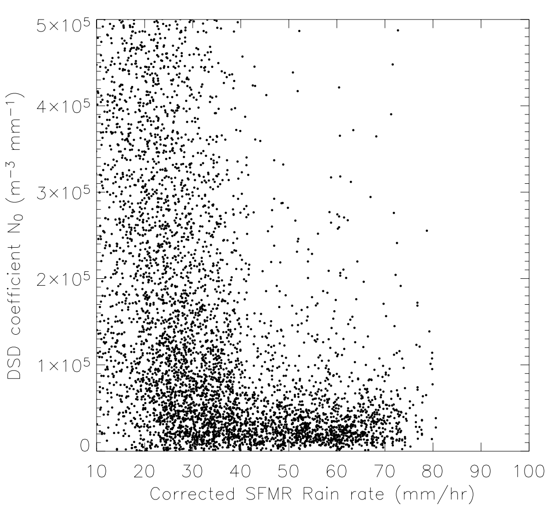

Fig. 6. Scatter plot of the N_0 coefficient, N_0, versus the corrected SFMR rainfall rate estimates obtained from the C-band 30 degrees incidence flight level reflectivity measurements acquired during the Isabel flights on the 12th, 13th and 14th of September.

VI. Acknowledgment

The authors would like to thank Jim McFadden, Sean McMillan, Jim Barr and all the other NOAA Aircraft Operation Center (AOC) personnel for their tremendous support during the Winter Experiments and Hurricane Seasons, well beyond their duties.

This work was supported by the Office of Naval Research (Remote Sensing) Grant N00014-01-1-0923, the National Oceanic and Atmospheric Administration Grant NA17EC1348 and the National Aeronautics and Space Administration Ocean Vector Winds Science Team.

References

[1] Esteban Fernandez, D., E. Kerr, A. Castells, S. Frasier, J. Carswell, P. Chang, P. Black, and F. Marks, "IWRAP: the Integrated Wind and Rain Airborne Profiler for remote sensing of the ocean and the atmospheric boundary layer within tropical cylones", to appear in *IEEE Trans. Geosci. Remote Sensing*, 2005.

[2] Uhlhorn, E.W., and P.G. Black, "Verification of remotely sensed sea surface winds in hurricanes", Journal of Atmospheric and Oceanic Technology, 20(1):99-116 (2003).

[3] Durden, S., E. Im, F.K. Li, R. Girard and K.S. Pak, "Surface Clutter Due to Antenna Sidelobes for Spaceborne Atmospheric Radar", *IEEE T. Geoscience Remote Sensing*, Vol. 39, No. 9, Sept, 2001., pp 1916-1921.

[4] Meneghini R. and T. Kozu, *Spaceborne Weather Radar*. Norwood, MA: Artch House, 1990.

[5] D. Atlas and C.W. Ulbrich, "Path- and area-integrated rainfall measurement by microwave attenuation in the 1-3 cm band", *Journal of Applied Meteorology*, vol. 16, pp. 1322–1331, 1977.

[6] Doviak, R.J., and Zrnic, D.S., *Doppler Radar and Weather Observations*, New Tork: Academic, 1984, 2nd edition.

[7] Jiang, H. "Quantitative Precipitation and Hydrometeor Content Estimation in Tropical Cyclones from Remote Sensing Observations", Ph.D. Thesis, University of Utah, 2003.

[8] Esteban Fernandez, D., "Remote Sensing of the Ocean and the Atmospheric Boundary Layer Within Tropical Cyclones", Ph.D. Thesis, University of Massachusetts, 2005.

[9] L.J. Battan, *Radar Observation of the Atmosphere*, University of Chicago Press, 1973.